Relation between Annular Modes and the Mean State: Southern Hemisphere Summer

FRANCIS CODRON

Laboratoire de Météorologie Dynamique du CNRS, Paris, France

(Manuscript received 7 March 2003, in final form 15 March 2004)

ABSTRACT

The annular modes emerge as the leading mode of extratropical month-to-month climate variability in both hemispheres. Here the influence of the background state on the structure and dynamics of the Southern Hemisphere annular mode (SAM) during the austral summer when the climatology is characterized by a single, well-defined, eddy-driven jet is studied. Subsets of the climatology are constructed for early and late summer, and for contrasting polarities of the ENSO cycle. The analysis is based both on observations and on perpetual-state GCM experiments. The main differences between the subsets involve variations of the latitude of the mean jet.

It is found that in all the cases, the SAM is characterized by latitudinal shifts of the jet about its mean position, reinforced by a positive momentum flux feedback from baroclinic waves. This result is consistent with previous studies of the dynamics of the zonally averaged circulation but is found here to hold over all longitudes and for different positions of the mean jet. The low frequency eddies exert a weaker negative feedback upon the mean flow, with a less zonally symmetric structure.

The strong differences in the amplitude of the SAM among the various climatologies seem to be determined by a combination of 1) the variance of the "random" forcing by transient eddies and 2) the strength of the positive feedback component of this forcing. The latter mechanism increases the variance at low frequencies only and lengthens the decorrelation time of zonal-mean zonal wind anomalies. It tends to become stronger when the mean jet moves equatorward.

1. Introduction

a. Previous work

It has long been known (Trenberth 1984; Karoly 1990, and the references therein) that much of the observed variability in the Southern Hemisphere midlatitudes projects on a zonally symmetric, vertically coherent pattern. More extensive recent work by Lorenz and Hartmann (2001, 2003), Limpasuvan and Hartmann (2000), Feldstein and Lee (1998), Feldstein (1998), and DeWeaver and Nigam (2000) focused on the variability of zonal-mean, in some cases vertically averaged, zonal wind or atmospheric angular momentum in the Northern or Southern Hemisphere. All of these studies confirmed that the most prominent mode exhibits a dipolar structure in zonal wind representing a north–south shift in the latitude of the eddy-driven jet. This jet shift mode has both a larger variance and longer persistence than the second mode, which represents an acceleration/tightening or deceleration/broadening of the jet.

The supposed dynamical origin of the prominence of such a mode is the interactions between the eddies and the zonal-mean flow; but there is still some debate concerning the relative importance of the various kinds of eddies. Lorenz and Hartmann (2001) find that the positive feedback from high-frequency eddies (or baroclinic waves) explains why the annular mode exhibits a substantial amount of variance at the lower frequencies. On the other hand, Feldstein and Lee (1998) find that, if baroclinic eddies randomly force zonal index fluctuations, their positive feedback is largely offset by the negative feedback from low and cross-frequency eddies.

Interest in the zonal index fluctuations grew after the observation by Thompson and Wallace (1998) that the first EOF of Northern Hemisphere sea level pressure [called the Arctic Oscillation (AO) or the Northern Annular Mode (NAM)] exhibits a strong zonally symmetric component. Although this mode is very similar to the North Atlantic Oscillation, its wider spatial extent suggests that its origin is not just regional. It may be the surface signature of hemispheric eddy–mean flow interaction, modified by the asymmetries imposed by mountains and ocean/land contrasts. This picture is supported by the many similarities between the Northern and the Southern Hemisphere annular modes, the latter having more pronounced zonal symmetry.

The definition of the NAM as an EOF has led to

Corresponding author address: Francis Codron, Laboratoire de Meteorologie Dynamique, T. 45–55, 3e E, Jussieu CNRS/UPMC, Boite 99, F-75252 Paris Cedex 05, France.
E-mail: fcodron@lmd.jussieu.fr

questioning of its physical meaning because the structure is not always recovered with different methods of data analysis (Ambaum et al. 2001) and, for example, the correlation between the Pacific and Atlantic Oceans centers of the NAM is weak. Ambaum et al. (2001) also argue that the relationship of the NAM with the climatological structures (like the mean jets) is different in the Pacific and Atlantic basins.

On the other hand, Quadrelli and Wallace (2002) recently observed that the structure of the NAM is somewhat different under different background conditions such as those observed during El Niño or La Niña events. Specifically, the correlation between the Atlantic and Pacific basins is found to be significant during the cold phase of the ENSO cycle.

A clarification of the relation between the annular modes and the climatology thus seems crucial for fully understanding their underlying dynamics and establishing them as physically relevant modes. It is also important to predict how they would behave under a changed climate.

b. Goal and approach

As a first step toward addressing these issues, we focus in this paper on the Southern Hemisphere annular mode (SAM) during summer and early fall because it represents the dynamically simplest case observable. During the austral summer season the midlatitude jetstream is, in fact, purely eddy driven, and no substantial stationary wave activity is observed.

We address the question of whether the annular mode is sensitive to changes in the climatological mean background state by studying the relation between the SAM wind anomalies and the mean jet for distinctively different mean states of the atmosphere, as defined by the opposing polarities of the ENSO cycle as well as by different months of year.

Our analysis is performed both on observations and on the output of perpetual-state GCM simulations. The two datasets are complementary: the observations from the National Centers for Environmental Prediction (NCEP) National Center for Atmospheric Research (NCAR), reanalysis are reliable in the Southern Hemisphere only for the last few decades. For the GCM, while some realism is sacrificed by using a model in equilibrium with constant forcing from the sun and with fixed SST, results with a very high level of statistical significance are obtained. The simulations are run for two different months of the climatology (January and March) and for three states with respect to ENSO (warm-El Niño, cold-La Niña, and normal conditions) to define six different background climatologies with constant model dynamics in which to explore the SAM variability.

Section 2 describes the data, analysis methods, and experimental setup used. The results related to the structure of the annular modes are presented in section 3. Section 4 is concerned with dynamical mechanisms and the role of eddy feedbacks in maintaining the annular mode. A discussion of the differences in the amplitude of the annular mode observed for the different basic states is given in section 5, and conclusions are given in the final section.

2. Analysis procedures

a. Methods

For both observations and model output the SAM is defined as the first principal component of Southern Hemisphere monthly 850-hPa geopotential height anomalies (poleward of 20°S), after weighting the data to account for the change of area with latitude. Each field presented is then obtained by a linear regression upon the standardized SAM time series. Monthly mean values are used throughout, except for some computations involving lagged regressions, for which daily values are used. Daily time series are constructed by projecting daily fields upon the spatial pattern obtained with SAM monthly values.

Daily values are also used to compute the eddy momentum flux convergence, or eddy forcing (EF)

$$\frac{1}{\cos^2\phi}\,\partial_y(\overline{u^*v^*}\cos^2\phi),$$

where ϕ is latitude, and the overbar and the star denote zonal average and departures from it, respectively. In some cases, daily wind speed values are first separated into high- and low-frequency components before computing the fluxes, using the filter described in Blackmon and Lau (1980) with a 10-day period cutoff.

b. Model experiments

For the model experiments the LMDZ3.3 version of the Laboratoire de Meteorologie Dynamique general circulation model has been used. It is a gridpoint model with 96 × 73 horizontal resolution, and 19 hybrid sigma–pressure coordinate levels in the vertical. More details can be found in Lott (1999). Overall, the model performance is comparable to other GCMs with similar resolution.

The GCM was run for six experiments, each 72 months in length, with constant solar radiation, SST, and sea ice boundary conditions. The first month of each run has not been included in our analysis in order to allow the model time to adjust from the initial state to its climatology.

The experiments are defined as follows: three have a perpetual 1 January insolation, three others a 1 March insolation. Each group of three is composed of a control run with climatological SSTs, a warm run, and a cold run. The El Niño (La Niña) experiments are defined by adding (subtracting) a two-standard-deviation ENSO-related SST anomaly to the climatology. The experiments with constant boundary conditions yield very stable statistics; in fact, the results presented below are

almost identical to those obtained in each half of the integrations.

The differences between the El Niño and La Niña mean simulated climates in the mid- and high latitudes are consistent with the observed differences: El Niño events are characterized by a strengthening and an equatorward shift of the jets and the associated storm tracks (Seager et al. 2003). The seasonal variation is another source of changes of the mean state: the jet shifts poleward in March compared to January.

From here onward, the simulations will be referred to as JW, J, and JC for perpetual January warm, neutral, and cold El Niño conditions, respectively, and MW, M, and MC for perpetual March.

c. Data

The observations used in this study are based on the NCEP–NCAR reanalysis dataset (Kalnay et al. 1996), from 1958 through 2001, on a 2.5° × 2.5° grid. For defining the state of the ENSO cycle we used the "cold tongue index" (CTI), defined as the SST anomalies (relative to the 1950–79 climatology, and with global mean SST removed) averaged over the area 6°N–6°S, 90°–180°W, based on the Comprehensive Ocean–

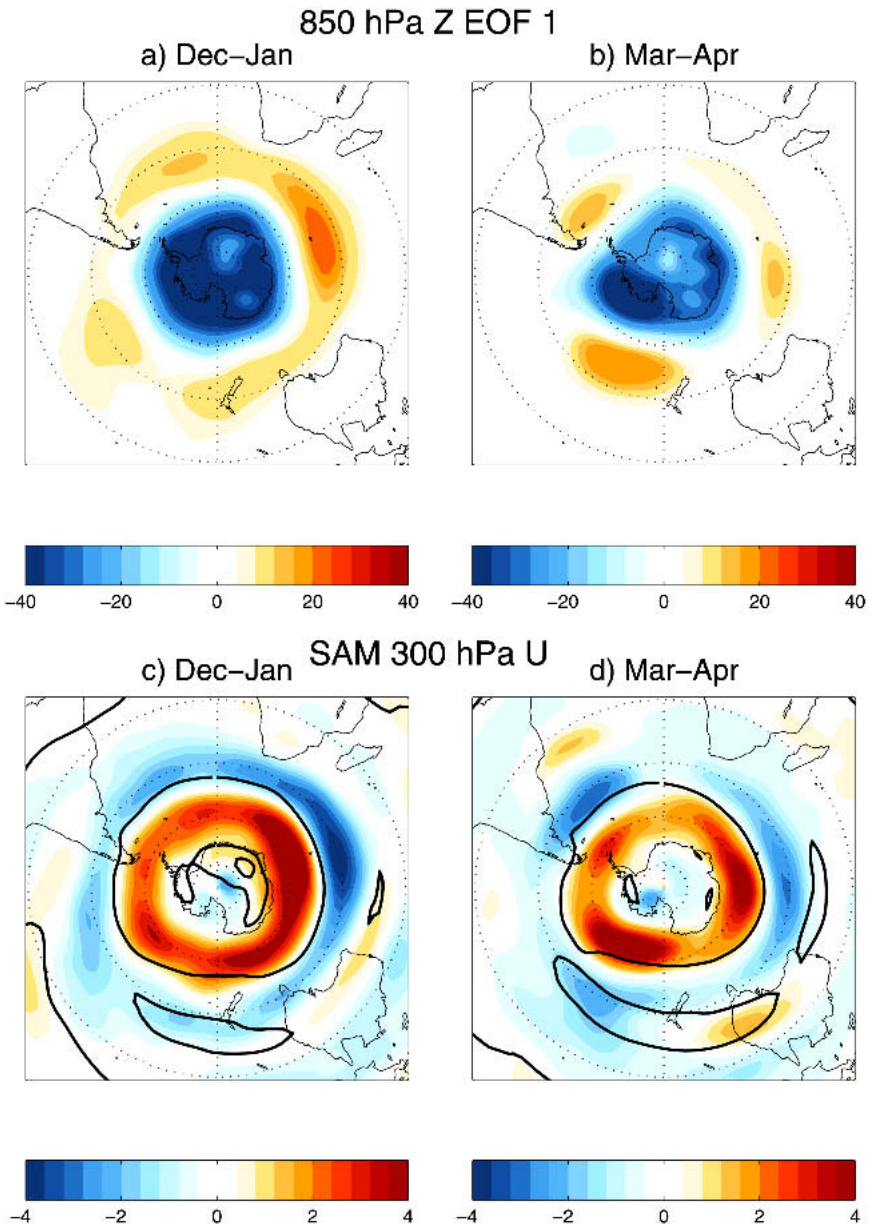

FIG. 1. NCEP–NCAR data regressed onto the standardized SAM time series. (a),(b) 850-hPa height (m); (c),(d) 300-hPa zonal wind (m s^{-1}). (a),(c) Dec–Jan; (b),(d) Mar–Apr. The black line indicates the extrema of the background mean zonal wind.

Atmosphere Dataset (COADS) described in Woodruff (2001a,b).

To define the two different mean states corresponding to the January and March integrations while retaining a substantial number of degrees of freedom, two 88-month subsets of the data are created by considering December–January (DJ) and March–April (MA) separately. The subsets are not further divided between El Niño and La Niña years, as was done for the GCM experiments, because the number of months would be too small to obtain stable statistics. Removing the ENSO signal has a very little impact on the SAM time series. The series obtained from data that include or do not include the ENSO signal are correlated with each other at a level above 0.98 in MA and 0.95 in DJ. The ENSO signature projects on the SAM structure (not shown) but with a small amplitude.

For daily values, a daily seasonal cycle is first computed after applying a 30-day running mean, then removed from the original data.

Since the reanalysis data are not very reliable in the Southern Hemisphere before 1979, we also repeated our analyses for the subset of the data extending from 1979 onward, and no significant differences were found.

3. Differences in SAM structure

a. Observations

The regression of the SAM onto 850-hPa geopotential height for the DJ and MA subsets of the NCEP–NCAR data is shown in Figs. 1a and 1b. The structure is roughly annular in both cases, although there are longitudinal variations in amplitude, especially for the MA subset.

The covarying upper-troposphere wind structure is shown in the bottom panels of Fig. 1 for the 300-hPa level, where the eddy-driven jet and the zonal index wind anomaly are strongest (Lorenz and Hartmann 2001). The strong correspondence between the node of the SAM signature and the maximum of the climatological jet (shown as a black line) indicates that at all longitudes the SAM represents a latitudinal shift of the jet. A small departure is observed around the date line, which coincides with the longitudinal sector in which a weak subtropical jet is also observed in the mean state.

To describe the latitudinal shifts of the SAM structure associated with changes in mean state, Fig. 2 compares the zonally averaged SAM wind U' with the mean meridional wind shear $\overline{U}_y$. For a latitude shift dy of the jet small enough compared to the width of the jet itself, the expected anomalous wind would be $U' = \partial\overline{U}/\partial y dy$.

Both subsets (DJ and MA) are consistent with this picture: the node of the SAM wind signature coincides with the zero crossing of the respective mean $\overline{U}_y$ profile and the entire meridional profiles of U' and $\overline{U}_y$ are very similar, with almost identical locations of the extrema. This relationship holds for the different mean states: the jet position is at a lower latitude in DJ, and this change is reflected in a more equatorward position of the DJ SAM signature compared to its MA counterpart.

Following Kushner et al. (2001), the latitude shift dy for one standard deviation of the SAM can be estimated by regressing U' on $\overline{U}_y$. The results in Table 1 show that a slightly higher variance is observed in DJ compared to MA.

Similar relationships between mean and anomalous wind are obtained for lower-tropospheric levels, in ac-

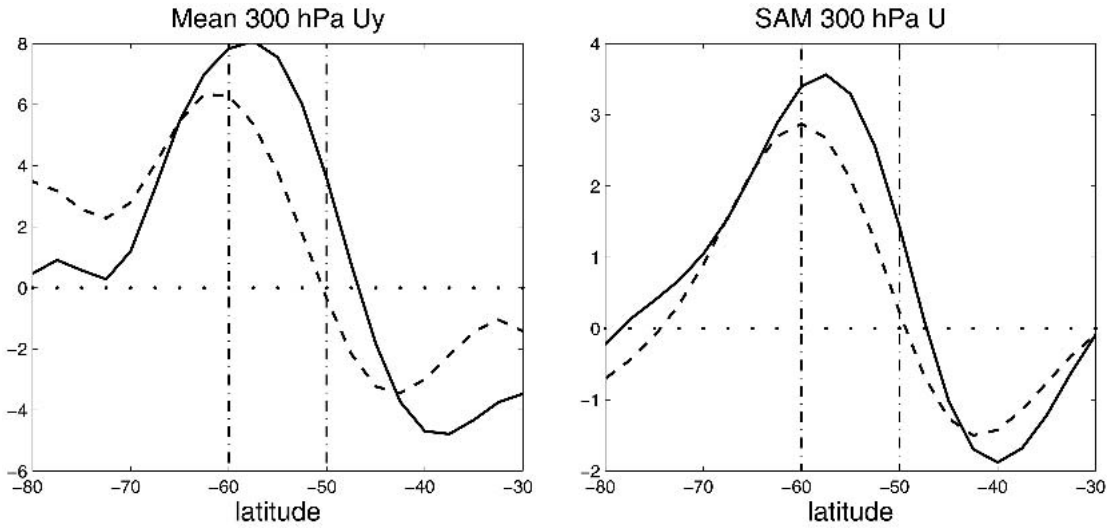

FIG. 2. NCEP–NCAR data: 300-hPa zonally averaged fields. (left) Meridional shear of climatological mean zonal wind [m s^{-1} (5°lat)$^{-1}$]. (right) Zonal wind regressed on SAM time series (m s^{-1}). Solid line: DJ, dashed line: MA. The vertical lines mark 50° and 60° lat.

TABLE 1. (left) Different simulations and (right) observations: mean jet latitude and *temporal* standard deviation (σ) of selected quantities associated with the SAM. Latitudes are in degrees, other units are arbitrary. The latitude of the mean jet decreases from left to right.

	MC	M	MW	JC	J	JW	MA	DJ
Mean jet latitude	49.5	48	43	39.5	36.5	35.5	50.5	47
Latitude shift (dy) σ	1.3	1.75	2.7	0.75	0.8	1	1.5	1.6
Eddy forcing σ	200	190	205	130	120	133	5.8	4.9

cordance with the known barotropic structure of the SAM.

b. GCM simulations

Figure 3 is the analog of Fig. 1 for each of the six GCM experiments. The latitudinal changes in the mean jet among the GCM simulations are larger than in the reanalysis subsets. Nevertheless, these diagrams confirm what was found in the observations: in each of the six simulations, the node of the SAM 300-hPa winds closely follows the mean jet position as it moves poleward from warm to cold ENSO conditions and from January to March.

It is interesting to note that the amplitudes, of the March El Niño SAM anomalies are twice as large as in any other of the six cases. The statistics on the latitude shift dy summarized in Table 1 confirm that the vari-

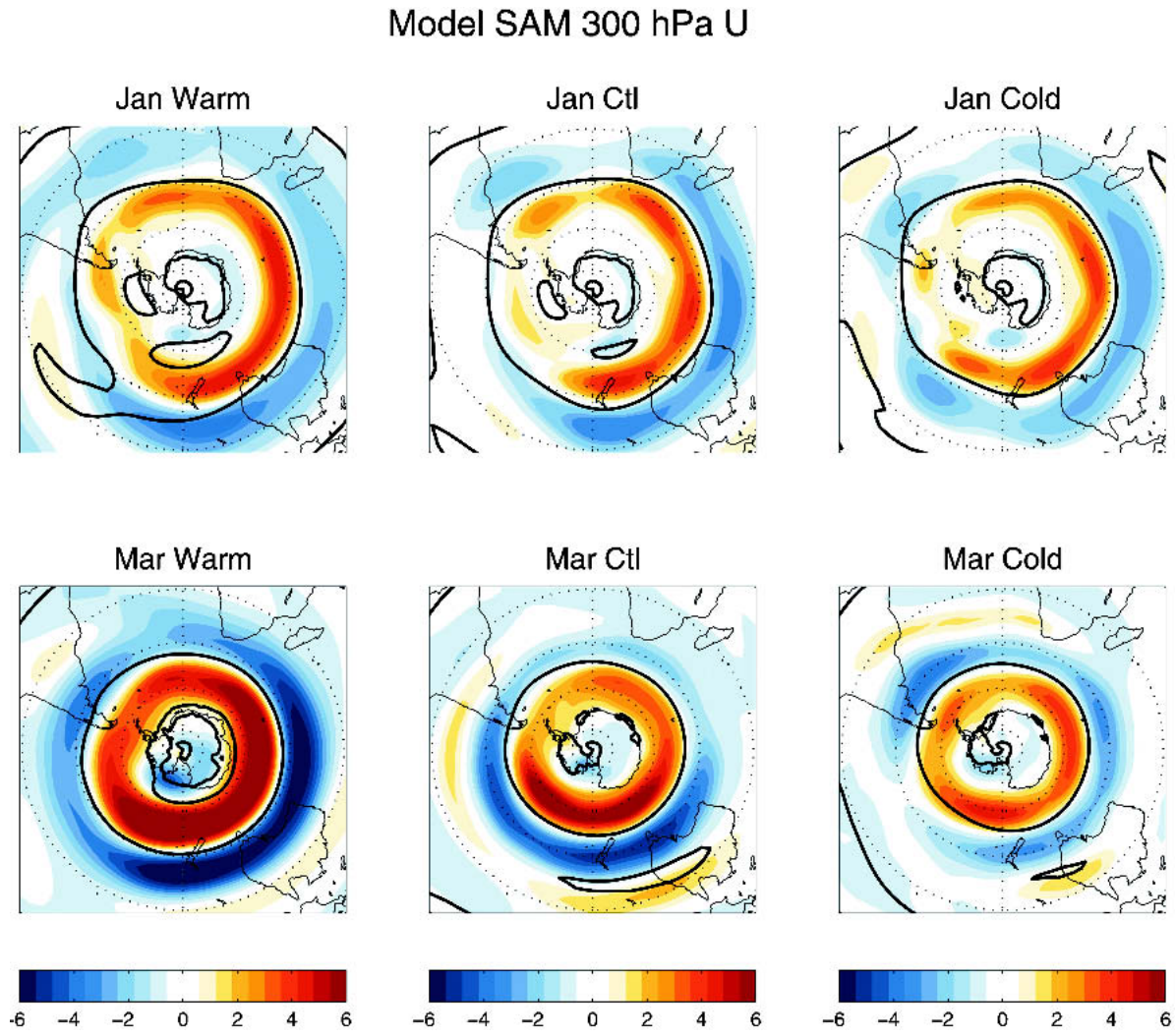

FIG. 3. GCM runs: 300-hPa zonal wind regressed upon the standardized SAM time series (m s^{-1}). The black lines denote the extrema of the mean zonal wind.

ability is generally larger in March than in January, and for warm than for cold conditions, thus higher in MW than in any other case.

Some possible explanations for these different amplitudes are discussed in section 5.

4. Dynamical mechanisms

Several authors (Lorenz and Hartmann 2001; Robinson 1996) showed that the prominence of the SAM is a consequence of positive feedback by high-frequency eddies on low-frequency mean flow anomalies. However, it is not obvious how to distinguish this feedback from random forcing of the SAM by the same eddies (Feldstein and Lee 1998).

We follow Lorenz and Hartmann (2001) by taking the eddy forcing at lags longer than its decorrelation time scale as the signature of a feedback.

For the six simulations, Fig. 4 shows the SAM zonal wind structure and its eddy feedback, represented by maps of momentum flux convergence by high-frequency (less than 10-day period) eddies (HFE) averaged over lags ranging from 5 to 20 days.

For all runs, the lagged HFE forcing exhibits a dipolar annular structure that tends to reinforce the SAM-related wind anomalies at all longitudes. In addition, both fields tend to have the highest amplitude in the same longitudinal sectors, although the correspondence is not perfect. In contrast, the low-frequency eddy (LFE) regression (not shown) does not exhibit a well-defined large-scale structure.

Figure 5 shows the latitudinal structure of the zonally averaged component of the same fields in more detail. The HFE positive feedback is evident, although its structure is narrower in latitude than the SAM wind anomalies. Hence, although in each case the poleward lobes of the SAM wind and HFE feedback are nearly coincident, for the equatorward part of the structure the EF is shifted poleward relative to the zonal wind anomalies. These relationships are consistent with an

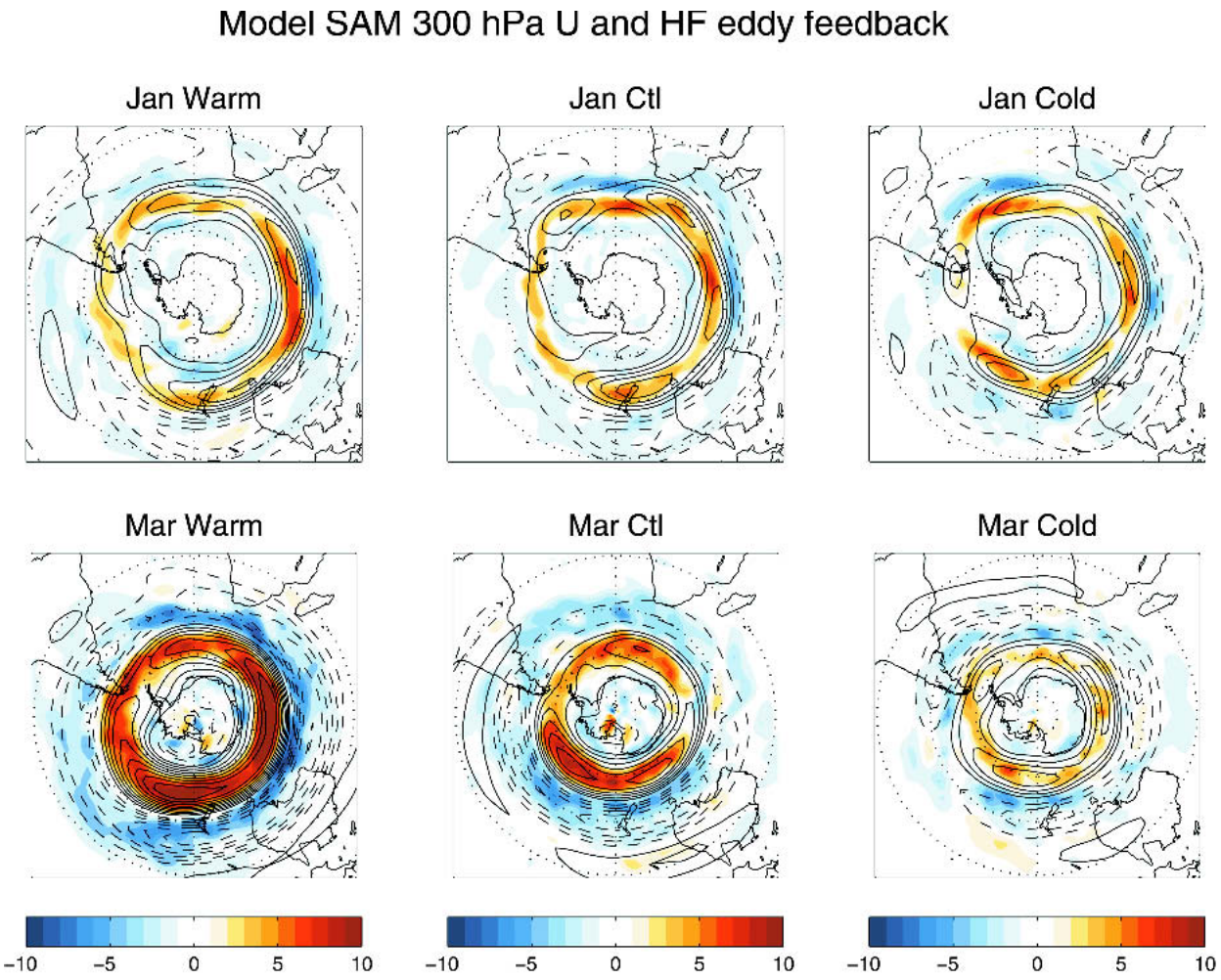

FIG. 4. GCM runs: 300-hPa fields regressed upon the standardized SAM time series. Zonal wind (contours; negative values dashed, interval 1 m s^{-1}) and lagged (5–20 days) HFE momentum flux convergence [color, $m^2\ s^{-2}\ (5°)^{-1}$].

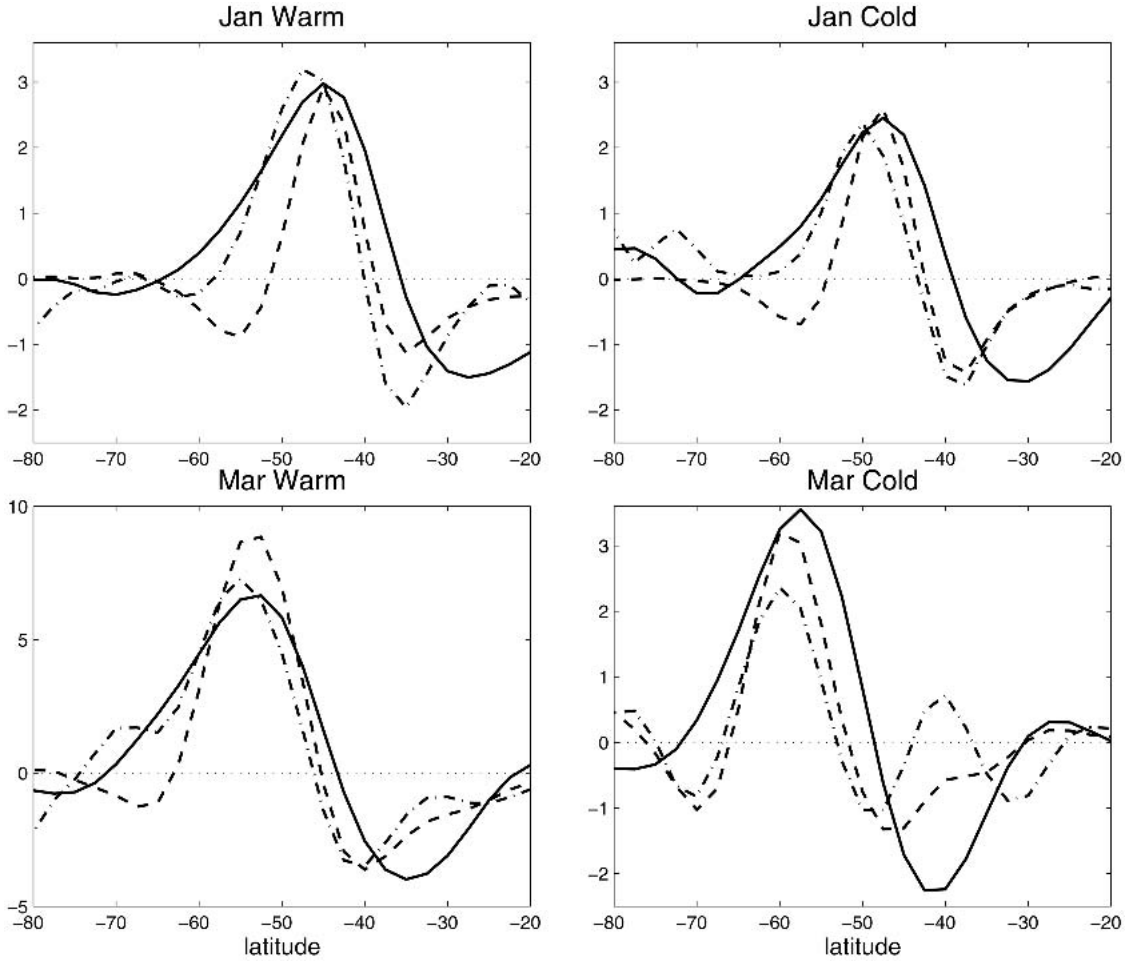

FIG. 5. GCM runs: 300-hPa zonally averaged fields regressed upon the standardized SAM time series. Zonal wind (solid, m s^{-1}), lagged HFE (dashed), and total eddies (dot–dashed) momentum flux convergence [m^2 s^{-2} $(5°)^{-1}$].

EF centered on average on the poleward flank of the mean jet, and shifting with the jet during a SAM event.

The effect of low frequency and cross-frequency eddies is generally to reduce the amplitude of the positive feedback, but never reversing it. Details vary considerably between different simulations.

The zonally averaged eddy feedback for observations is shown in Fig. 6. As in the simulations, the poleward lobe of the HFE feedback follows the SAM. However, the amplitude of the total eddy feedback is weaker than in the GCM, mostly due to the stronger negative contribution of LFE.

5. Differences in SAM variance

We try now to quantify the importance of the eddy feedback and to explain the differences in the SAM variance observed in the simulations, especially the very large variance of the March warm conditions.

We use daily time series of the zonally averaged zonal wind and EF, both projected onto the monthly zonal wind anomaly pattern. Figure 7 shows lagged autocorrelation of zonal wind, and its cross-correlation with EF, for several of the GCM simulations.

The cross-correlation is always maximal when EF leads by a few days, in agreement with the idea of the SAM being randomly forced by eddies. The correlation drops when the eddies immediately lag the SAM. This drop is due to the negative cross-correlation of the LFE and, in fact, disappears when only HFEs are considered (not shown).

The most interesting feature is the positive correlation at lags of up to 30 days. It is a signature of a positive eddy feedback (Lorenz and Hartmann 2001) and reinforces the results of the previous section. This correlation increases in all cases when only HFE forcing is considered (not shown).

Large differences are observed among the simulations. Higher lagged EF correlations correspond to a lower SAM wind decorrelation time, consistent with the idea of feedback. The SAM persistence is highest for MW and lowest for MC. It is also higher for JW than

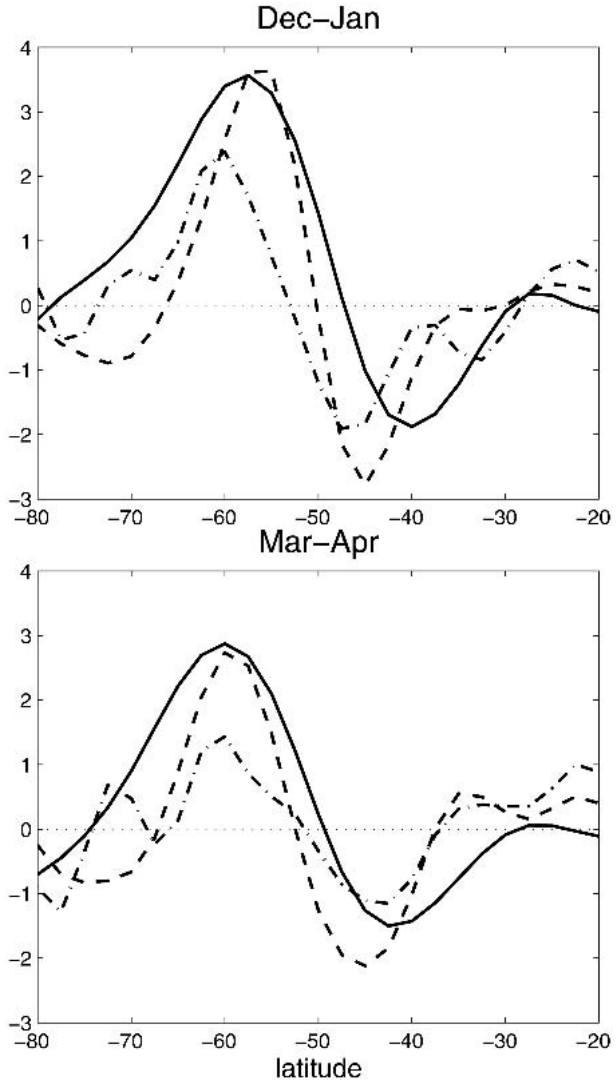

FIG. 6. NCEP data: 300-hPa zonally averaged fields regressed upon the standardized SAM time series. Zonal wind (solid, m s^{-1}), and lagged (5–20 days) HFE (dashed), and total eddies (dot–dashed) momentum flux convergence [m^2 s^{-2} $(5°)^{-1}$]: (top) DJ, (bottom) MA.

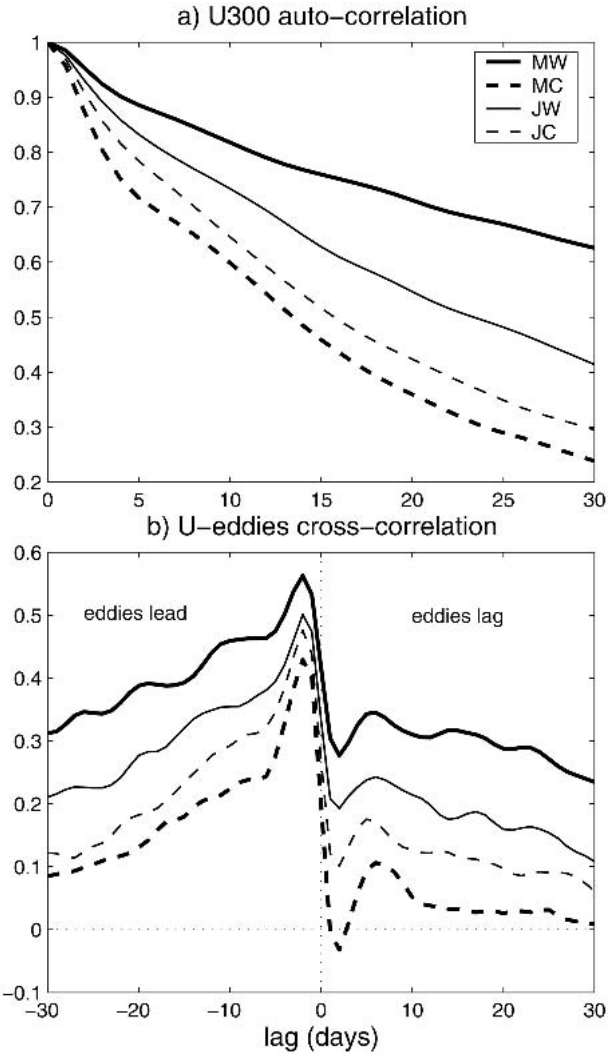

FIG. 7. GCM runs SAM 300-hPa zonally averaged zonal wind: (a) autocorrelation, (b) cross-correlation with eddy forcing. March: thick lines, January: thin lines. Warm: continuous lines, cold: dashed lines; normal conditions omitted.

for JC. The J and M simulations (not shown) are intermediate between the corresponding respective warm and cold cases.

However, the SAM amplitude (Table 1) does not simply follow the order suggested by Fig. 7 (stronger feedback yielding higher variance). The SAM variance is, in fact, always higher for warm than for cold conditions, but higher for MC than for any January simulation despite the weaker feedback by eddies in this case.

This apparent contradiction can be resolved by noting in Table 1 that the total variance of the EF is always much larger in March than in January. Thus, the stronger overall eddy forcing more than compensates for the weaker eddy feedback.

The different effects of total eddy forcing and feedback are apparent when looking at the power spectra of the SAM wind and EF (Fig. 8). The power is virtually identical for warm and cold conditions, either in January or March, except at the lowest frequencies. However, it is much higher in March than in January because of the larger EF amplitude. At the very low frequencies, the eddy feedback becomes dominant (Lorenz and Hartmann 2001), and the variance for MC becomes much lower than for MW. A smaller difference is also seen between JW and JC.

An attempt to quantify more precisely the effects of eddies is presented in Table 2. For each simulation, the amplitudes of lagged EF and wind anomalies are compared, and their pattern correlation is computed.

The differences in the strength of the feedback could

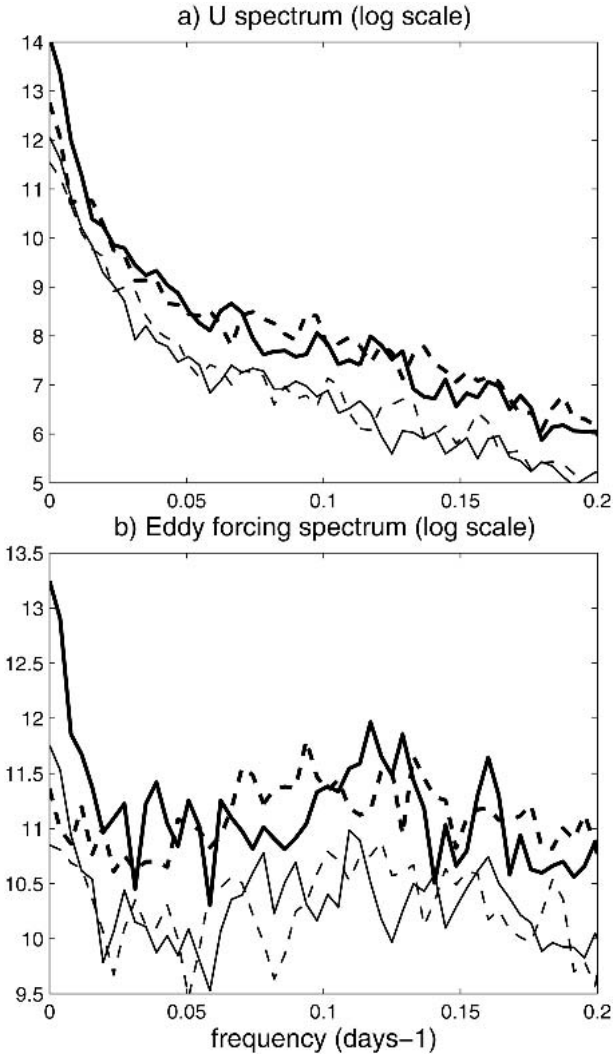

FIG. 8. Spectra of time series of 300-hPa zonal-mean fields projected upon the SAM zonal wind pattern: (a) zonal wind, (b) total eddy forcing. March: thick lines, January: thin lines. Warm: continuous, cold: dashed; normal conditions omitted. Logarithmic scale.

be due to differences in the strength of the lagged EF response or to the degree to which it projects on the wind anomaly pattern, but only the latter factor can explain the longer persistence of the March warm run.

In the observations (Table 1) the SAM exhibits a slightly higher variance in DJ (confirmed by other measures of the SAM variance). However, the EF is stronger in MA. The previous discussion would suggest that this discrepancy can be explained by the stronger feedback in DJ, which would enhance the low-frequency variability in particular. This is indeed the case, as evidenced by Fig. 9, which shows that the persistence of SAM anomalies and the lagged correlation with EF are significantly stronger in DJ than in MA.

As for the simulated cases, Table 2 suggests that both the amplitude of eddy feedback and the pattern correlation with wind anomalies contribute to the longer persistence.

6. Conclusions and discussion

We have analyzed the structure of the Southern Hemisphere annular mode for different phases of ENSO and the seasonal cycle, using both observations and GCM output. These different mean states all have a well-defined eddy-driven jet, the latitude of which varies from one climatology to the next, leading to different adaptations of the SAM.

The different cases share a number of common features:

- Even without any prior zonal averaging, the SAM has a pronounced zonally symmetric structure. It is equivalent barotropic in the vertical and corresponds at all longitudes to a meridional shift of the jet about its mean position.
- The response of the momentum flux by HFE at the 300-hPa level yields a positive feedback for the SAM. This result is consistent with previous studies of the zonally averaged momentum balance. In particular, although the model overestimates the strength of the feedback, the detailed features of the time analysis of the simulations, such as the shape of the eddy spectra and the cross-correlation with the wind anomalies, are remarkably similar to the observational results of Lorenz and Hartmann (2001). The strong similarity between the structure of the observed and simulated results lends confidence to the model results.
- The structure of the HFE feedback is very zonal: it is positive at all longitudes. It tends to be stronger where the wind anomalies are also stronger, suggesting the possibility of local control of the amplitude.

These points are valid for each of the six flow configurations that we have examined in the GCM experiments and for the two seasons in the NCEP–NCAR

TABLE 2. Comparison for (left) simulations and (right) observations of the relative amplitudes (measured as *spatial* standard deviation σ) and the pattern correlation of lagged eddy forcing (EF) and zonal wind anomalies. EF is averaged over lags from 5–20 days. Correlation coefficients are dimensionless, other units are arbitrary. The latitude of the mean jet decreases from left to right.

	MC	M	MW	JC	J	JW	MA	DJ
EF/SAM amplitude $\sigma(\overline{u'v'_y})/\sigma(U')$	.54	.83	.92	.82	.88	.92	.31	.33
EF–SAM pattern correlation $(U'\ \overline{u'v'_y})/\sigma(U')\ \sigma(\overline{u'v'_y})$	.45	.71	.85	.63	.66	.74	.56	.58

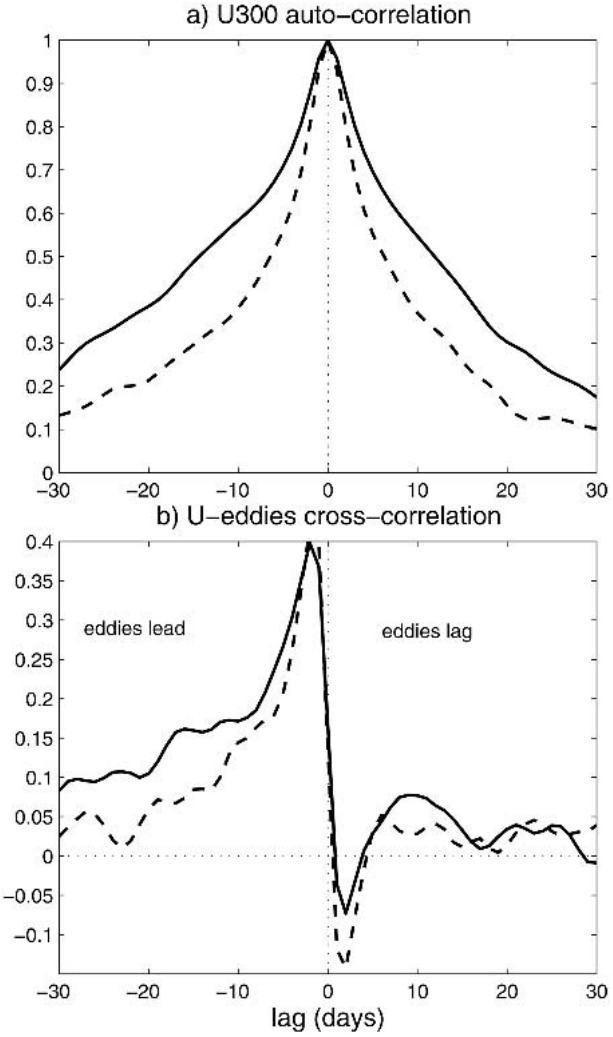

FIG. 9. NCEP–NCAR data: (a) SAM 300-hPa wind autocorrelation, (b) cross-correlation of wind with eddy forcing. DJ: continuous line, MA: dashed line.

reanalyses. They are consistent with the idea that the prominence of the leading EOF derives from a positive feedback from the transient eddies. This feedback is not strong enough to cause the zonal wind anomalies to grow, but it acts against dissipation, thereby increasing the persistence of zonal wind anomalies and increasing their variance.

However, the eddy feedback is not the only factor controlling the SAM variance. The amplitude of the "random" component of the eddy forcing (i.e., the component not organized by the mean flow) is found to be equally important. This second factor explains why the simulated SAM variability is larger in the March cold case than in all January conditions (despite the weaker MC feedback). Both factors contribute to the very large SAM amplitude observed in the March warm case.

There are important dynamical differences between these two mechanisms. First, changes in the intensity of the random forcing influence the variance on all time scales, whereas the feedback by organized eddies enhances specifically low frequency variability. It can also "select" a preferred structure: Lorenz and Hartmann (2001, 2003) found that the prominence of EOF1 relative to EOF2 is due to the fact that the feedback of EOF1 tends to reinforce the zonal wind anomalies, whereas the feedback from EOF2 tends to move them poleward.

All other things being equal, we find that the feedback is stronger when the mean jet is displaced toward the equator. This is true for either January or March simulations (shifting from cold to warm conditions), as well as for observations (shifting from MA to DJ). Although no explanation can be singled out at this time, there are several factors that could conceivably contribute:

- The jet becomes more baroclinic as it moves equatorward. Thus, a shift in latitude would imply smaller surface wind anomalies and a weaker damping of the SAM by the surface drag. The Coriolis parameter appears twice in this mechanism, first in the strength of the secondary meridional circulation induced by upper-level zonal wind anomalies, and also in the efficiency of this secondary circulation in transporting momentum to the surface layer (through the Coriolis torque terms).
- The propagation characteristics of the waves are different under different mean conditions. It is essential that baroclinic waves be able to propagate away from the source region in order to yield a positive feedback (Robinson 2000).
- The impact of low frequency eddies also appears important.

Work in progress is aimed at studying how the SAM evolves under more complex configurations of the mean state (i.e., the simultaneous presence of eddy-driven and subtropical jets, and stationary waves).

A major conclusion of our study is that the annular mode does not exhibit a structure fixed in space. Both the shape and the dynamics can be modified by even modest changes of the background state. The important implication for climate change studies is that the dominant patterns of variability observed in the present climate cannot be considered "stationary" in future and past climates. This idea should also be kept in mind when reconstructing indexes of past climate variability.

Acknowledgments. The numerical experiments were performed at the Institut de Recherches en Informatique Scientifique (IDRIS). Most of the research was done during a visit at the Joint Institute for Study of Atmosphere and Ocean of the University of Washington. The author would like to thank David Lorenz, Roberta Quadrelli, and especially John. M. Wallace for useful discussions and his help in preparing the manuscript.

REFERENCES

Ambaum, M. H. P., B. J. Hoskins, and D. B. Stephenson, 2001: Arctic oscillation or North Atlantic oscillation? *J. Climate,* **14,** 3495–3507.

Blackmon, M. L., and N.-C. Lau, 1980: Regional characteristics of the northern hemisphere wintertime circulation: A comparison of the simulation of a GFDL general circulation model with observations. *J. Atmos. Sci.,* **37,** 497–514.

DeWeaver, E., and S. Nigam, 2000: Do stationary waves drive the zonal-mean jet anomalies of the northern winter? *J. Climate,* **13,** 2160–2176.

Feldstein, S., 1998: The growth and decay of low-frequency anomalies in a GCM. *J. Atmos. Sci.,* **55,** 415–428.

——, and S. Lee, 1998: Is the atmospheric zonal index driven by an eddy feedback? *J. Atmos. Sci.,* **55,** 3077–3086.

Kalnay, E., and Coauthors, 1996: The NCEP/NCAR 40-Year Reanalysis Project. *Bull. Amer. Meteor. Soc.,* **77,** 437–471.

Karoly, D. J., 1990: The role of transient eddies in low-frequency zonal variations of the Southern Hemisphere circulation. *Tellus,* **42A,** 41–50.

Kushner, P. J., I. M. Held, and T. L. Delworth, 2001: Southern Hemisphere atmospheric circulation response to global warming. *J. Climate,* **14,** 2238–2249.

Limpasuvan, V., and D. L. Hartmann, 2000: Wave-maintained annular modes of climate variability. *J. Climate,* **13,** 4414–4429.

Lorenz, D. J., and D. L. Hartmann, 2001: Eddy–zonal flow feedback in the Southern Hemisphere. *J. Atmos. Sci.,* **58,** 3312–3327.

——, and ——, 2003: Eddy–zonal flow feedback in the Northern Hemisphere winter. *J. Climate,* **16,** 1212–1227.

Lott, F., 1999: Alleviation of stationary biases in a GCM through a mountain drag parameterization scheme and a simple representation of mountain lift forces. *Mon. Wea. Rev.,* **127,** 788–801.

Quadrelli, R., and J. M. Wallace, 2002: Dependence of the structure of the Northern Hemisphere annular mode on the polarity of ENSO. *Geophys. Res. Lett.,* **29,** 2132, doi:10.102a/2002GL015807.

Robinson, W. A., 1996: Does eddy feedback sustain variability in the zonal index? *J. Atmos. Sci.,* **53,** 3556–3569.

——, 2000: A baroclinic mechanism for the eddy feedback on the zonal index. *J. Atmos. Sci.,* **57,** 415–422.

Seager, R., N. Harnik, Y. Kushnir, W. Robinson, and J. Miller, 2003: Mechanisms of hemispherically symmetric climate variability. *J. Climate,* **16,** 2960–2978.

Thompson, D. W. J., and J. M. Wallace, 1998: The Arctic Oscillation signature in the wintertime geopotential height and temperature fields. *Geophys. Res. Lett.,* **25,** 1297–1300.

Trenberth, K. E., 1984: Interannual variability of the Southem Hemisphere circulation: Representativeness of the year of the global weather experiment. *Mon. Wea. Rev.,* **112,** 108–123.

Woodruff, S. D., 2001a: COADS updates including newly digitized data and the blend with the UK Meteorological Office Marine Data Bank. *Proc. Workshop on Preparation, Processing and Use of Historical Marine Meteorological Data,* Tokyo, Japan, Japan Meteorological Agency and the Ship & Ocean Foundation, 9–13.

——, 2001b: Quality control in recent COADS updates. *Proc. Workshop on Preparation, Processing and Use of Historical Marine Meteorological Data,* Tokyo, Japan, Japan Meteorological Agency and the Ship & Ocean Foundation, 49–53.